












A constraint on historic growth in global photosynthesis due to rising CO₂

Received: 13 October 2022

Accepted: 18 October 2023

Published online: 27 November 2023

 Check for updates

T. F. Keenan ^{1,2}✉, X. Luo ^{1,2,3}, B. D. Stocker ^{4,5,6,7,8}, M. G. De Kauwe ^{9,10,11},
B. E. Medlyn ¹², I. C. Prentice ^{13,14,15}, N. G. Smith ¹⁶, C. Terrer ¹⁷, H. Wang ¹⁵,
Y. Zhang ^{1,2,18} & S. Zhou ^{1,2,19,20,21,22}

Theory predicts that rising CO₂ increases global photosynthesis, a process known as CO₂ fertilization, and that this is responsible for much of the current terrestrial carbon sink. The estimated magnitude of the historic CO₂ fertilization, however, differs by an order of magnitude between long-term proxies, remote sensing-based estimates and terrestrial biosphere models. Here we constrain the likely historic effect of CO₂ on global photosynthesis by combining terrestrial biosphere models, ecological optimality theory, remote sensing approaches and an emergent constraint based on global carbon budget estimates. Our analysis suggests that CO₂ fertilization increased global annual terrestrial photosynthesis by $13.5 \pm 3.5\%$ or 15.9 ± 2.9 PgC (mean \pm s.d.) between 1981 and 2020. Our results help resolve conflicting estimates of the historic sensitivity of global terrestrial photosynthesis to CO₂ and highlight the large impact anthropogenic emissions have had on ecosystems worldwide.

Globally, photosynthesis results in the single largest flux of carbon dioxide (CO₂) between the atmosphere and the biosphere^{1,2}. Long-term changes in photosynthesis, for example in response to rising atmospheric CO₂, could therefore provide an important feedback to climate change^{3–5}. Global terrestrial photosynthetic carbon uptake cannot be observed directly, however, and must instead be either predicted by terrestrial biosphere models (TBMs) or inferred from proxies². The multiple long-term proxies from which changes in global terrestrial photosynthesis are

derived include satellite-based estimates^{6,7}, ice-core records of carbonyl sulfide (COS)⁸ and herbarium samples of deuterium isotopomers⁹, along with information gleaned from the seasonal cycle of atmospheric CO₂ (ref. 10). Despite the importance of photosynthesis, however, and the multiple proxies that exist, there is no consensus about the expected historic change in terrestrial photosynthesis due to rising CO₂ (refs. 3–12).

Satellite-based estimates of global terrestrial photosynthetic carbon uptake are derived from observations of spatiotemporal variations in

¹Department of Environmental Science, Policy and Management, UC Berkeley, Berkeley, CA, USA. ²Climate and Ecosystem Sciences Division, Lawrence Berkeley National Laboratory, Berkeley, CA, USA. ³Department of Geography, National University of Singapore, Singapore, Singapore. ⁴Institute of Geography, University of Bern, Bern, Germany. ⁵Department of Environmental Systems Science, ETH, Zürich, Switzerland. ⁶Swiss Federal Institute for Forest, Snow and Landscape Research WSL, Birmensdorf, Switzerland. ⁷Institute of Geography, University of Bern, Bern, Switzerland. ⁸Oeschger Centre for Climate Change Research, University of Bern, Bern, Switzerland. ⁹School of Biological Sciences, University of Bristol, Bristol, UK. ¹⁰ARC Centre of Excellence for Climate Extremes, Sydney, New South Wales, Australia. ¹¹Climate Change Research Centre, University of New South Wales, Sydney, New South Wales, Australia. ¹²Hawkesbury Institute for the Environment, Western Sydney University, Penrith, New South Wales, Australia. ¹³Department of Life Sciences, Imperial College London, Ascot, UK. ¹⁴Department of Biological Sciences, Macquarie University, North Ryde, New South Wales, Australia. ¹⁵Department of Earth System Science, Tsinghua University, Haidian, Beijing, China. ¹⁶Department of Biological Sciences, Texas Tech University, Lubbock, TX, USA. ¹⁷Department of Civil and Environmental Engineering, Massachusetts Institute of Technology, Cambridge, MA, USA. ¹⁸Sino-French Institute for Earth System Science, College of Urban and Environmental Sciences, Peking University, Beijing, China. ¹⁹Lamont-Doherty Earth Observatory of Columbia University, Palisades, NY, USA. ²⁰Earth Institute, Columbia University, New York, NY, USA. ²¹Department of Earth and Environmental Engineering, Columbia University, New York, NY, USA. ²²State Key Laboratory of Earth Surface Processes and Resources Ecology, Faculty of Geographical Science, Beijing Normal University, Beijing, China. ✉e-mail: trevorkeen@berkeley.edu

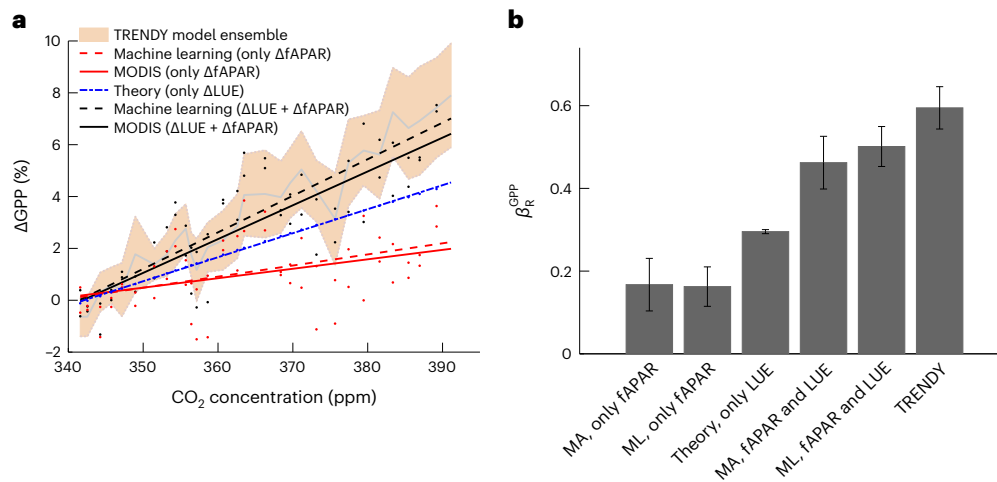


Fig. 1 | Long-term changes in global annual photosynthesis from TBMs and multiple satellite observations. a, Relative changes in global terrestrial photosynthesis (ΔGPP , %) from 1982 ($\text{CO}_2 = 341$ ppm) to 2012 ($\text{CO}_2 = 391$ ppm) based on simulations from process-based models in the TRENDY project model ensemble (orange, mean \pm s.d.) and two different satellite approaches (empirical MODIS algorithm (MA, solid lines); a machine learning method (ML, dashed lines)). Estimates from the satellite approaches were obtained allowing for an effect of increasing CO_2 on either the fAPAR (red lines, dots), the LUE of

photosynthesis (blue line) or both fAPAR and LUE (black lines, dots). **b**, Inferred CO_2 sensitivities (β_R^{GPP} ; Methods) from the data presented in **a**, for the standard satellite-based approaches using ML and the MODIS algorithm (MA) with the CO_2 effect on GPP manifest through changes in fAPAR, the modified MA approach with a CO_2 effect only on LUE (MA, only LUE) and both ML and MA satellite RS-based approaches with an effect of increasing CO_2 on both LUE and fAPAR. Black error bars represent the mean standard error of β_R^{GPP} for each product (MA, ML) or the mean standard error across TRENDY models.

surface reflectance, from which vegetation solar energy absorption can be derived. As they integrate land surface observations, they are often regarded as a benchmark to which TBMs should be compared¹¹. Such comparisons generally suggest that TBMs overestimate the change in global terrestrial photosynthesis due to too high a sensitivity of photosynthesis to increasing CO_2 (refs. 6,11). However, satellite–TBM comparisons are mired by the fact that most satellite-based estimates, be they machine learning (ML) or algorithmically based, do not incorporate the universally observed direct effect of increasing CO_2 on the light-use efficiency (LUE) of leaves of C_3 vegetation¹³. This is because the direct effect of increasing CO_2 on LUE is not directly observable from space¹⁴. In contrast, observation-based proxies, based on ice-core records of COS^{8,15}, eddy-covariance networks¹² and herbarium and field-based deuterium isotopomers⁹, suggest that TBMs may underestimate the sensitivity of global photosynthesis to CO_2 . TBMs themselves show a large range of sensitivities of global terrestrial photosynthesis to CO_2 (refs. 10,16,17), though few demonstrate sensitivities as low as the average satellite-inferred values^{6,14} or typically as high as those derived from the COS or deuterium proxies^{8,9,17}. The spread in estimates of the sensitivity of global terrestrial photosynthesis to CO_2 and the lack of a global constraint, constitutes a large source of uncertainty in future projections of the Earth system¹⁸ and hinders attribution of the various processes responsible for long-term changes in the global terrestrial carbon cycle.

Here, we use remote sensing (RS) observations informed with ecological optimality theory to help constrain the historic response of photosynthesis to rising CO_2 . We develop a method to incorporate the direct effect of CO_2 on the rate of canopy-level terrestrial gross primary photosynthesis (GPP) in established satellite-based approaches. We do so using first-principles theory of photosynthetic carbon fixation^{19,20} and generate 30-year global datasets of satellite-derived GPP. In addition, we identify an emergent multimodel relationship^{21–23} between the modelled terrestrial carbon sink and the sensitivity of photosynthesis to CO_2 from the Trends in Net Land–Atmosphere Carbon Exchanges project (TRENDY²⁴). When combined, these approaches constrain the range of plausible estimates of the historic effect of CO_2 on global GPP, resolving the large apparent difference between

satellite- and TBM-inferred sensitivities of GPP to historic changes in atmospheric CO_2 .

We reconciled the apparent difference between the TBM-inferred and satellite-based estimates of the sensitivity of GPP to CO_2 (Fig. 1) by using first-principles theory to incorporate the direct effect of increasing CO_2 on C_3 LUE in the satellite-based estimates. We refer to RS estimates that incorporate theory of the direct effect of CO_2 on LUE as the modified RS-based methods hereafter. The direct effect of CO_2 on LUE reflects the increasing competitiveness of CO_2 relative to O_2 for the active sites of the ribulose-1,5-bisphosphate carboxylase-oxygenase (RuBisCO) enzyme and the increasing competitiveness of CO_2 as atmospheric concentrations rise (Methods). To do so we considered two distinct classes of satellite-based estimates. The first is a commonly used LUE approach based on the Moderate Resolution Imaging Spectroradiometer (MODIS) algorithm (the MA approach) and the second is an ML approach that integrates both satellite and ground observations of ecosystem carbon fluxes. The direct effect of increasing CO_2 on the LUE of canopy photosynthesis¹³ was roughly twice as large as the indirect effect of increasing canopy leaf area and thus increasing the fraction of absorbed photosynthetically active radiation (fAPAR), represented in the ML and MA approaches (Fig. 1a,b). The long-term sensitivity of the RS-based estimates of GPP modified to account for both the direct (β_R^{LUE}) and indirect (β_R^{fAPAR}) effect of increasing CO_2 (β_R^{GPP} ; equation (1)) was 0.50 ± 0.1 (mean \pm s.d.) and 0.46 ± 0.1 for the ML and MA approaches, respectively (Fig. 1b), compared to 0.16 ± 0.05 and 0.16 ± 0.06 for the original ML and MA-based estimates, respectively (Fig. 1b). The long-term increase in GPP from the updated RS-based estimates thus more closely approximated that of the TBM ensemble mean ($\beta_R^{\text{GPP}} = 0.59 \pm 0.16$) (Fig. 1b). The modified RS-based methods predict a $7.27 \pm 0.7\%$ (ML) and $6.72 \pm 0.9\%$ (MA) increase in global annual GPP for a 14.5% increase in atmospheric CO_2 between 1982 and 2012.

Despite the agreement between the updated satellite methods and the TBM model ensemble (Fig. 1b), there is a large spread in individual TBM sensitivities and the true sensitivity is uncertain because of the lack of a comparable observational record. To address this issue, we proposed a constraint on the historic response of

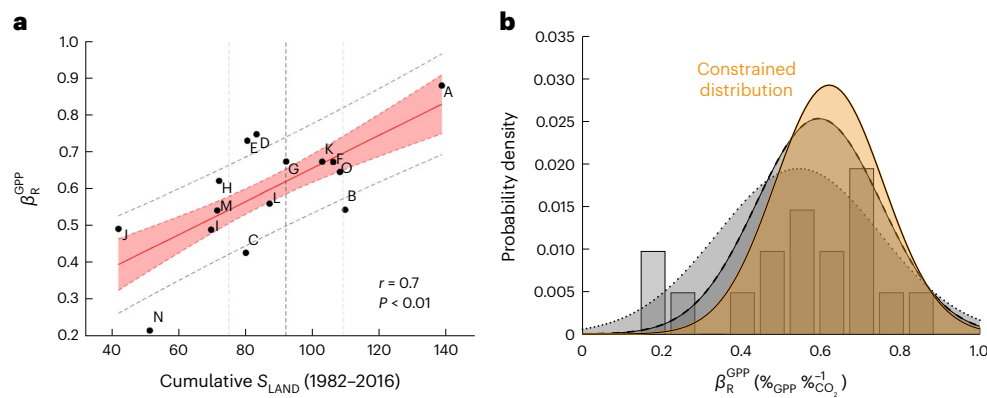


Fig. 2 | A constraint on the sensitivity of global terrestrial photosynthesis to CO₂. **a**, The relationship between the modelled sensitivity of GPP to CO₂ (β_R^{GPP} , TRENDY experiment S1: dynamic CO₂ only) and the modelled cumulative terrestrial carbon sink (PgC, TRENDY experiment S3: dynamic CO₂, climate and land use). Individual TRENDY model details and β_R^{GPP} values are listed in Supplementary Table 2. The red line and shaded area show the best linear fit across models and the associated prediction standard error (dashed red) and standard deviation of prediction error (dashed grey) intervals. The vertical

dashed lines shows the cumulative residual terrestrial carbon sink (mean, s.d.) between 1982 and 2016 as estimated by the Global Carbon Project²⁷. **b**, The unconstrained probability density function (PDF) distribution of β_R^{GPP} across all original estimates (TRENDY models and the original RS-based approaches; dotted line, grey bars) and the unconstrained PDF of β_R^{GPP} across the TRENDY TBMs (dashed black line). The orange area represents the conditional probability distribution derived by applying the constraint from **a** to the model ensemble.

photosynthesis to rising CO₂ by combining the TRENDY modelled sensitivity of global GPP, for which no direct observations exist, with the magnitude of the cumulative global terrestrial residual carbon sink between 1982 and 2016 (S_{LAND}), for which there are constrained estimates^{25,26}. Using cumulative S_{LAND} estimates as opposed to shorter time periods reduces the influence of annual or decadal random error. Model sensitivities of photosynthesis to CO₂ (Supplementary Table 2) were positively correlated ($r = 0.70$, $P < 0.01$) with the magnitude of the modelled cumulative terrestrial sink on a multidecadal scale (Fig. 2a), with a stronger CO₂ fertilization effect leading to a larger modelled cumulative sink. This emergent relationship^{21–23}, provides an opportunity to constrain the wide range in estimates of the sensitivity of GPP to CO₂ with the observed magnitude of S_{LAND} , particularly when combined with the results of the modified RS-based estimates. The full distribution, which includes the TBMs (Supplementary Table 2) and the original RS-based estimates, provides an estimate of β_R^{GPP} of 0.54 ± 0.21 (mean \pm s.d.; Fig. 2b), which is lower than that derived from the distribution of TBMs ($\beta_R^{\text{GPP}} = 0.59 \pm 0.16$). The posterior TBM distribution, formed by bootstrapping the cumulative land-sink emergent constraint relationship (Fig. 2a) provides a constrained estimate of β_R^{GPP} of 0.62 ± 0.14 (Fig. 2b). This is 30% lower than the maximum unconstrained estimate and over 200% higher than that of the original RS-based approaches. The constrained distribution represents a 33% reduction in uncertainty compared to the full distribution of β_R^{GPP} (Fig. 2b) and a 13.5% reduction compared to the unconstrained TBM ensemble (Fig. 2b).

Results from the updated RS estimates and the emergent constraint provide a point of comparison for other reported estimates of the sensitivity of global terrestrial photosynthesis to CO₂. A long-term COS proxy has been proposed⁸, which simulates photosynthetic change on the basis of a mass balance of global COS sources and sinks from 1900 to 2013 and suggests an increase in photosynthesis equivalent to an effective β_R^{GPP} of 0.94 (Supplementary Table 1). This is comparable to the highest sensitivity of the TBM models used here¹⁷. The COS estimate, however, integrates over a longer time period and therefore potentially captures changes in the land surface unrelated to CO₂, such as reforestation and the agricultural green revolution²⁷, and is thus not directly comparable to the emergent constraint and updated RS estimates presented here. Another proxy, based on deuterium isotopomers gathered from herbarium specimens and field trials⁹, suggests an historic change equivalent to a β_R^{GPP} of 1.03

(Supplementary Table 1). Although higher than that derived from COS, the deuterium isotopomer estimate reflects the effect of increasing CO₂ on photosynthesis for leaves in full sunlight. As shaded leaves experience stronger light limitation, which results in a lower sensitivity to CO₂, COS-based estimates could thus reasonably be expected to be higher than the canopy integrated sensitivity. Our results indicate that such large implied sensitivities are probably overestimates (Fig. 2).

The closer agreement between the updated RS approaches and the TBMs (Fig. 1) allows for their response to CO₂ to be probed more deeply. The sensitivity of C₃ photosynthesis to CO₂ increases strongly with temperature²⁸ (Fig. 3a; equations (2)–(7)) because the suppression of oxygenation by RuBisCO with increasing CO₂ is greater at higher temperatures. Reduced RuBisCO oxygenation reduces photorespiration at high temperatures, as represented by the temperature dependence of the photosynthetic CO₂ compensation point (Γ^* , equation (3)). The resulting latitudinal gradient is reproduced by both the TBMs examined (Fig. 3b) and the updated RS approaches (Fig. 3c–e). The results indicate that the influence of CO₂ on photosynthesis at high latitudes is limited due to low temperatures. Estimates of the long-term change in GPP from the updated RS approaches show large changes, particularly in areas of intensive agriculture such as the midwestern United States, central and northern Europe and India (Fig. 3c,d). Compared to the RS approaches (Fig. 3d), the TBMs predict smaller increases in arid mid- and low-latitude regions, particularly in Australia and South Africa but much larger increases in the productive croplands and tropical and temperate forests (Fig. 3d). The lower TBM sensitivity, in particular of shrublands (Fig. 3f), is potentially due to poorly represented TBM processes such as the positive relationship between CO₂ and woody shrub expansion²⁹. The lower TBM sensitivities could be from inaccurate representation of greening trends that arise from changes in land management practices such as reforestation³⁰. The relatively higher TBM sensitivity regions, particularly tropical forests (Fig. 3), may be due to insufficient TBM representation of nutrient constraints³¹, or the saturation of RS vegetation indices at high leaf area³², reflecting large uncertainty about the response of tropical forest photosynthesis to CO₂ (ref. 33). In general, the magnitude of the TBM and updated satellite β_R^{GPP} suggests that the global terrestrial photosynthetic response to CO₂ is consistent with the response of the light-limited photosynthetic rate which has also been suggested by observations of photosynthesis and biomass changes at the ecosystem scale^{34–36}, theoretical models^{37,38} and by model results showing that

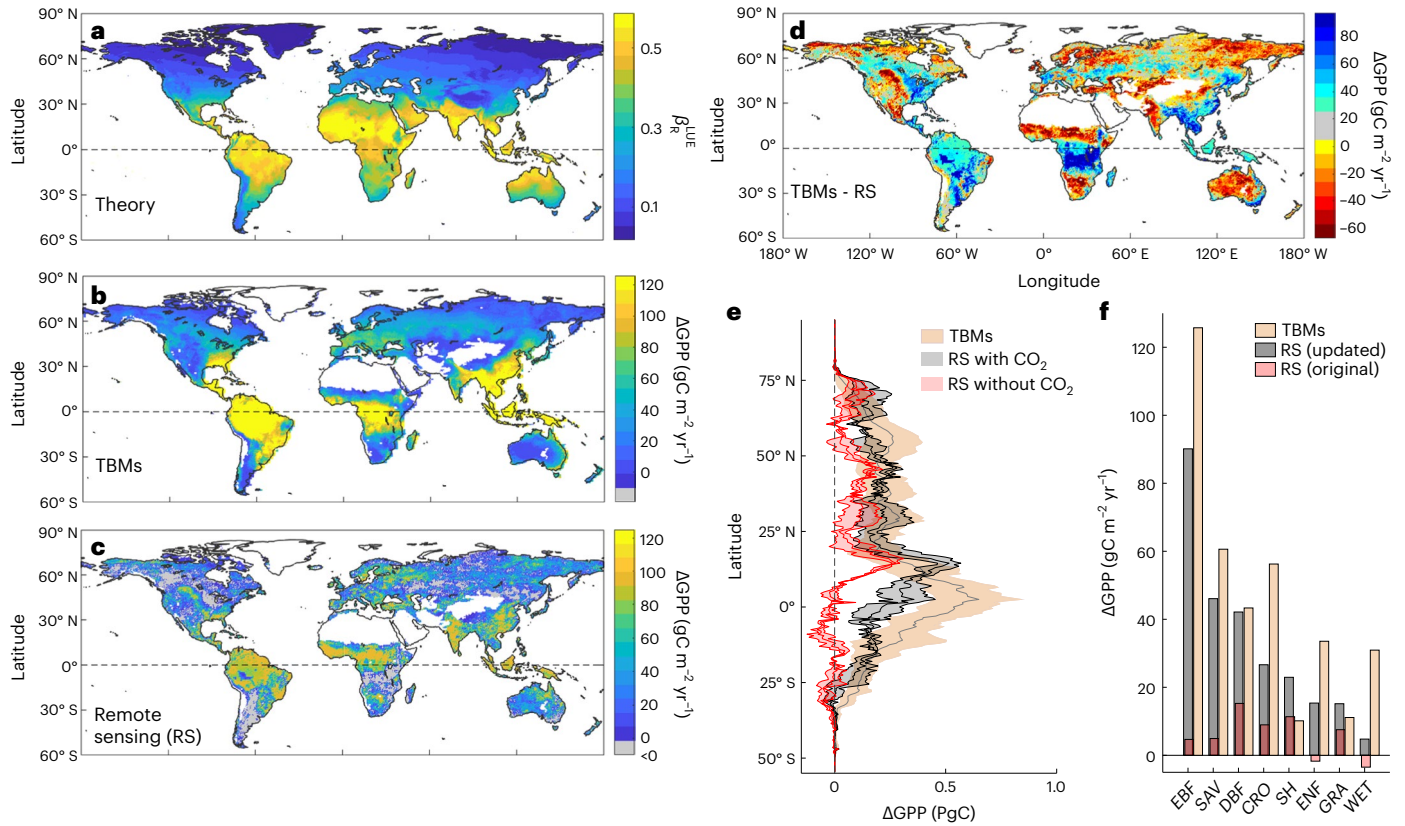


Fig. 3 | Spatial differences in the estimated long-term changes in global terrestrial photosynthesis from LUE theory, TBMs and satellite observations combined with theory. a–f. The global distribution of: the sensitivity of terrestrial photosynthesis on a leaf area basis to CO₂ (β_R^{LUE}) due to changes in LUE (a); CO₂-induced changes in terrestrial photosynthesis (ΔGPP , gC m⁻² yr⁻¹) from 1982 to 2012 from an ensemble of TBMs (TBMs; TRENDY-S1) (b); mean long-term changes in GPP from the two updated satellite methods, which includes a modelled direct (β_R^{LUE}) and measured indirect (β_R^{fAPAR}) effect of increasing CO₂ on GPP, in addition to the effect of land use and climate changes on the fraction of

absorbed radiation (fAPAR) (c); the difference between the data presented in b and c (d); the latitudinal distribution of long-term changes in gross primary photosynthesis (ΔGPP , PgC) from 1982 to 2012, from the TBM ensemble (orange shaded area, mean, s.d. across models) and ΔGPP predicted from RS approaches with (black, mean, s.d. between MODIS and ML approaches) and without (red) a direct effect of CO₂ on LUE (Methods) (e); and long-term changes in ΔGPP , separated by plant functional types (f). EBF, evergreen broadleaved forest; SAV, savanna; DBF, deciduous broadleaved forests; CRO, croplands; SH, shrublands; ENF, evergreen needleleaf forests; GRA, grasslands; WET, wetlands.

electron-transport limited leaves are responsible for most global carbon assimilated through photosynthesis³⁹.

As with any application of the emergent constraint technique, it is important to highlight that many factors could lead to biases and undermine the robustness of the derived constraint. Of primary concern is the potential for emergent constraints to rely on spurious cross-model correlations that are not based on a clear physical relationship⁴⁰. The constraint we identify is based on the relationship between CO₂ and the land sink, for which there is ample observational and theoretical support^{3,4}. Although CO₂ fertilization is by no means the sole likely reason for an increasing land sink⁴ (other contributions arise from forest regrowth, nitrogen fertilization, growing season extensions and release from cold limitations), such processes are included in the models examined and contribute to the scatter in the relationship between β_R^{GPP} and S_{LAND} presented in Fig. 2a. That said, there are many processes inadequately represented in both TBMs and the satellite approaches that could lead to biases in the derived β_R^{GPP} . For example, models have been shown to poorly reproduce changes in the seasonal cycle of atmospheric CO₂ (ref. 41) and demonstrate a range of responses when compared to results from experimental manipulation⁴². Nutrient limitation, thermal temperature acclimation, water stress, disturbances (including land-use change) and leaf area dynamics are all poorly represented in TBMs^{42,43}. Future implementations of new process representations or model structures may lead to updated inference on the response of photosynthesis to CO₂.

A further source of uncertainty relates to the degree of structural similarity between models and the potential for systematic cross-model biases. For example, if all models in the ensemble had the same missing or biased process representation, which led to systematic bias in the modelled relationship between the sensitivity of photosynthesis to CO₂ and the land sink across models, that could bias the emergent constraint reported here. Systematic cross-model biases with shared structural similarity could also lead to an underestimation of the uncertainty associated with the values derived from the emergent constraint^{40,44}.

The models we examine represent the state-of-the-science for land surface modelling and have substantial diversity of process representations and responses to forcings⁴⁵, even for well-studied processes such as photosynthesis. Because of this diversity, there are outlier models with high or low CO₂ sensitivities or S_{LAND} estimates and such ‘wrong’ models are necessary for the formation of an emergent constraint. Indeed, removal of some outlier models, in particular CABLE and VEGAS, degrades the derived relationship between β_R^{GPP} and S_{LAND} presented in Fig. 2a (to $r = 0.5, 0.64; P = 0.03, 0.01$, respectively) and removal of both models leads to no statistically significant relationship between β_R^{GPP} and S_{LAND} ($P = 0.15$). If future versions of current outlier models are more consistent with the ensemble, the constraint identified here may no longer be evident.

Global photosynthesis is the largest flux of CO₂ in the global carbon cycle and small changes in terrestrial photosynthesis over time can lead to large changes in the net carbon sink. The resulting feedback from the

effect of increasing CO₂ on photosynthesis (the carbon–concentration feedback) has been estimated to be over four times larger and more uncertain, than the direct carbon–climate feedback⁴⁶. The large differences between estimates of historic changes in GPP^{6–10,15} are therefore disconcerting and could potentially lead to incorrect inference about biases in current TBMs^{6,14} and long-term changes in related components of the global carbon cycle such as soil respiration^{11,47}. The confluence of approaches we use bounds the plausible range of the historic effect of CO₂ on global terrestrial photosynthesis to a β_R^{GPP} of 0.62 ± 0.14 (mean, s.d.; Fig. 2b) and helps to reconcile differences in previous estimates. The results also show that widely used RS-based estimates of global terrestrial photosynthesis need to incorporate the effect of increasing CO₂ on photosynthetic LUE and provide a globally applicable approach that is broadly consistent with the TBMs examined. Together, our results suggest that increases in atmospheric CO₂ have led to a large increase in global photosynthesis since 1982, representing a strong carbon–concentration feedback that has helped to slow down the accumulation of anthropogenic emissions in the atmosphere.

Online content

Any methods, additional references, Nature Portfolio reporting summaries, source data, extended data, supplementary information, acknowledgements, peer review information; details of author contributions and competing interests; and statements of data and code availability are available at <https://doi.org/10.1038/s41558-023-01867-2>.

References

- Keenan, T. F. & Williams, C. A. The terrestrial carbon sink. *Annu. Rev. Environ. Resour.* **43**, 219–243 (2018).
- Ryu, Y., Berry, J. A. & Baldocchi, D. D. What is global photosynthesis? History, uncertainties and opportunities. *Remote Sens. Environ.* **223**, 95–114 (2019).
- Walker, A. P. et al. Integrating the evidence for a terrestrial carbon sink caused by increasing atmospheric CO₂. *New Phytol.* <https://doi.org/10.1111/nph.16866> (2020).
- Ruehr, S. et al. Evidence and attribution of the enhanced land carbon sink. *Nat. Rev. Earth Environ.* **4**, 518–534 (2023).
- Schimel, D., Stephens, B. B. & Fisher, J. B. Effect of increasing CO₂ on the terrestrial carbon cycle. *Proc. Natl Acad. Sci. USA* **112**, 436–441 (2015).
- Smith, W. K. et al. Large divergence of satellite and Earth system model estimates of global terrestrial CO₂ fertilization. *Nat. Clim. Change* **6**, 306–310 (2016).
- Sun, Z. et al. Evaluating and comparing remote sensing terrestrial GPP models for their response to climate variability and CO₂ trends. *Sci. Total Environ.* **668**, 696–713 (2019).
- Campbell, J. E. et al. Large historical growth in global terrestrial gross primary production. *Nature* **544**, 84–87 (2017).
- Ehlers, I. et al. Detecting long-term metabolic shifts using isotopomers: CO₂-driven suppression of photorespiration in C₃ plants over the 20th century. *Proc. Natl Acad. Sci. USA* <https://doi.org/10.1073/pnas.1504493112> (2015).
- Wenzel, S., Cox, P. M., Eyring, V. & Friedlingstein, P. Projected land photosynthesis constrained by changes in the seasonal cycle of atmospheric CO₂. *Nature* **538**, 499–501 (2016).
- Li, W. et al. Recent changes in global photosynthesis and terrestrial ecosystem respiration constrained from multiple observations. *Geophys. Res. Lett.* **45**, 1058–1068 (2018).
- Chen, C., Riley, W. J., Prentice, I. C. & Keenan, T. F. CO₂ fertilization of terrestrial photosynthesis inferred from site to global scales. *Proc. Natl Acad. Sci. USA* **119**, e2115627119 (2022).
- Ainsworth, E. A. & Long, S. P. What have we learned from 15 years of free-air CO₂ enrichment (FACE)? A meta-analytic review of the responses of photosynthesis, canopy properties and plant production to rising CO₂. *New Phytol.* **165**, 351–372 (2005).
- De Kauwe, M. G., Keenan, T. F., Medlyn, B. E., Prentice, I. C. & Terrer, C. Satellite based estimates underestimate the effect of CO₂ fertilization on net primary productivity. *Nat. Clim. Change* **6**, 892–893 (2016).
- Cernusak, L. A. et al. Robust response of terrestrial plants to rising CO₂. *Trends Plant Sci.* **24**, 578–586 (2019).
- Piao, S. et al. Evaluation of terrestrial carbon cycle models for their response to climate variability and to CO₂ trends. *Glob. Change Biol.* **19**, 2117–2132 (2013).
- Haverd, V. et al. Higher than expected CO₂ fertilization inferred from leaf to global observations. *Glob. Change Biol.* **26**, 2390–2402 (2020).
- Friedlingstein, P. et al. Uncertainties in CMIP5 climate projections due to carbon cycle feedbacks. *J. Clim.* **27**, 511–526 (2014).
- Prentice, I. C., Dong, N., Gleason, S. M., Maire, V. & Wright, I. J. Balancing the costs of carbon gain and water transport: testing a new theoretical framework for plant functional ecology. *Ecol. Lett.* **17**, 82–91 (2014).
- Keenan, T. F. et al. Recent pause in the growth rate of atmospheric CO₂ due to enhanced terrestrial carbon uptake. *Nat. Commun.* **7**, 13428 (2016).
- Eyring, V. et al. Taking climate model evaluation to the next level. *Nat. Clim. Change* **9**, 102–110 (2019).
- Winkler, A. J., Myneni, R. B. & Brovkin, V. Investigating the applicability of emergent constraints. *Earth Syst. Dynam.* **10**, 501–523 (2019).
- Hall, A., Cox, P., Huntingford, C. & Klein, S. Progressing emergent constraints on future climate change. *Nat. Clim. Change* **9**, 269–278 (2019).
- Sitch, S. et al. Recent trends and drivers of regional sources and sinks of carbon dioxide. *Biogeosciences* **12**, 653–679 (2015).
- Friedlingstein, P. et al. Global Carbon Budget 2021. *Earth Syst. Sci. Data* **14**, 1917–2005 (2022).
- Joos, F., Meyer, R., Bruno, M. & Leuenberger, M. The variability in the carbon sinks as reconstructed for the last 1000 years. *Geophys. Res. Lett.* **26**, 1437–1440 (1999).
- Zeng, N. et al. Agricultural Green Revolution as a driver of increasing atmospheric CO₂ seasonal amplitude. *Nature* **515**, 394–397 (2014).
- Long, S. P. Modification of the response of photosynthetic productivity to rising temperature by atmospheric CO₂ concentrations: has its importance been underestimated? *Plant Cell Environ.* **14**, 729–739 (1991).
- Stevens, N., Lehmann, C. E. R., Murphy, B. P. & Durigan, G. Savanna woody encroachment is widespread across three continents. *Glob. Change Biol.* **23**, 235–244 (2017).
- Chen, C. et al. China and India lead in greening of the world through land-use management. *Nat. Sustain.* **2**, 122–129 (2019).
- Fleischer, K. et al. Amazon forest response to CO₂ fertilization dependent on plant phosphorus acquisition. *Nat. Geosci.* **12**, 736–741 (2019).
- Myneni, R. B. et al. Global products of vegetation leaf area and fraction absorbed PAR from year one of MODIS data. *Remote Sens. Environ.* **83**, 214–231 (2002).
- Cernusak, L. A. et al. Tropical forest responses to increasing atmospheric CO₂: current knowledge and opportunities for future research. *Funct. Plant Biol.* **40**, 531–551 (2013).
- Ainsworth, E. A. & Rogers, A. The response of photosynthesis and stomatal conductance to rising [CO₂]: mechanisms and environmental interactions. *Plant Cell Environ.* **30**, 258–70 (2007).
- Baig, S., Medlyn, B. E., Mercado, L. M. & Zaehle, S. Does the growth response of woody plants to elevated CO₂ increase with temperature? A model-oriented meta-analysis. *Glob. Change Biol.* **21**, 4303–4319 (2015).

36. Yang, J. et al. Low sensitivity of gross primary production to elevated CO₂ in a mature eucalypt woodland. *Biogeosciences* **17**, 265–279 (2020).
37. McMurtrie, R. E., Comins, H. N., Kirschbaum, M. U. F. & Wang, Y. P. Modifying existing forest growth models to take account of effects of elevated CO₂. *Aust. J. Bot.* **40**, 657–677 (1992).
38. Luo, Y., Sims, D. A., Thomas, R. B., Tissue, D. T. & Ball, J. T. Sensitivity of leaf photosynthesis to CO₂ concentration is an invariant function for C₃ plants: a test with experimental data and global applications. *Glob. Biogeochem. Cycles* **10**, 209–222 (1996).
39. Li, Q. et al. Leaf area index identified as a major source of variability in modeled CO₂ fertilization. *Biogeosciences* **15**, 6909–6925 (2018).
40. Williamson, M. S. et al. Emergent constraints on climate sensitivities. *Rev. Mod. Phys.* **93**, 025004 (2021).
41. Graven, H. D. et al. Enhanced seasonal exchange of CO₂ by Northern ecosystems since 1960. *Science* **341**, 1085–1089 (2013).
42. Zaehle, S. et al. Evaluation of 11 terrestrial carbon–nitrogen cycle models against observations from two temperate free-air CO₂ enrichment studies. *New Phytol.* **202**, 803–822 (2014).
43. De Kauwe, M. G. et al. Where does the carbon go? A model-data intercomparison of vegetation carbon allocation and turnover processes at two temperate forest free-air CO₂ enrichment sites. *New Phytol.* **203**, 883–899 (2014).
44. Sanderson, B. et al. On structural errors in emergent constraints. *Earth Syst. Dynam. Discuss.* <https://doi.org/10.5194/esd-2020-85> (2021).
45. Fisher, J. B., Huntzinger, D. N., Schwalm, C. R. & Sitch, S. Modeling the terrestrial biosphere. *Annu. Rev. Environ. Resour.* **39**, 91–123 (2014).
46. Arora, V. K. et al. Carbon–concentration and carbon–climate feedbacks in CMIP5 earth system models. *J. Clim.* **26**, 5289–5314 (2013).
47. Ballantyne, A. et al. Accelerating net terrestrial carbon uptake during the warming hiatus due to reduced respiration. *Nat. Clim. Change* **7**, 148–152 (2017).

Publisher's note Springer Nature remains neutral with regard to jurisdictional claims in published maps and institutional affiliations.

Open Access This article is licensed under a Creative Commons Attribution 4.0 International License, which permits use, sharing, adaptation, distribution and reproduction in any medium or format, as long as you give appropriate credit to the original author(s) and the source, provide a link to the Creative Commons license, and indicate if changes were made. The images or other third party material in this article are included in the article's Creative Commons license, unless indicated otherwise in a credit line to the material. If material is not included in the article's Creative Commons license and your intended use is not permitted by statutory regulation or exceeds the permitted use, you will need to obtain permission directly from the copyright holder. To view a copy of this license, visit <http://creativecommons.org/licenses/by/4.0/>.

© The Author(s) 2023

Methods

The β metric of CO₂ sensitivity

We quantified the apparent sensitivity of global terrestrial GPP to CO₂ in the RS, TBM and independent proxy estimates using two approaches: (1) the percentage change in GPP with respect to GPP at the start of the time period (equation (5) below) and (2) a β metric defined as the response ratio (R) of GPP with respect to CO₂:

$$\beta_R = \frac{[\text{GPP}(t) - \text{GPP}(t_0)] / \text{GPP}(t_0)}{[\text{Ca}(t) - \text{Ca}(t_0)] / \text{Ca}(t_0)} \quad (1)$$

where $\text{GPP}(t)$ is the value of GPP at time t and $\text{Ca}(t)$ is the value of atmospheric [CO₂] at time t . Although other methods to calculate the β -factor have been proposed (for example, ref. 48), we use equation (1) for ease of interpretation. A β of 1 represents direct proportionality between the GPP CO₂ response and the change in CO₂. Note that to avoid undue influence of year-to-year variability in GPP, we estimated $\text{GPP}(t)$ and $\text{GPP}(t_0)$ on the basis of a linear regression fit to the GPP time series.

Assessing the CO₂-sensitivity of satellite-based GPP

Recent reports have highlighted that the most commonly used satellite-based estimates of GPP have a much lower CO₂-sensitivity than that derived from TBMs^{6,11}. However, most satellite-based estimates do not incorporate the universally observed direct effect of increasing CO₂ on the LUE of leaves of C₃ vegetation¹³, which is not observable from space¹⁴. The effect of increasing CO₂ on global terrestrial C₃ photosynthesis that we examine here manifests through two primary pathways: though increasing the biochemical rate of photosynthesis on a leaf area basis⁴⁹, which we refer to as the direct effect and through increases in leaf area on a ground area basis, allowing for the interception of greater amounts of light^{50,51}, which we refer to as the indirect effect. The former, direct response, arises because CO₂ is a substrate for the photosynthetic enzyme, RuBisCO. Both CO₂ and O₂ compete at the active site of RuBisCO, so changes in the concentration of either affect the rate at which CO₂ is assimilated, effectively changing the LUE of photosynthesis on a leaf area basis at a given light level. The latter, indirect response of increasing leaf area index (LAI⁵¹) and the resulting increase in the (fAPAR), reflects both the increased carbon available to invest in structural growth under elevated CO₂ and potential changes in the hydrological equilibrium due to elevated CO₂-induced increases in water-use efficiency, which can lead to increased leaf area in water-limited ecosystems^{52–54}. Both response pathways are incorporated in TBMs²⁴ and long-term proxies account for each to differing degrees. Most satellite-based estimates, however, do not account for the direct effect of increasing CO₂ on the biochemical rate of photosynthesis^{14,55}.

We assessed whether incorporating a CO₂ sensitivity of LUE in RS-based approaches for estimating GPP reconciled the difference between the sensitivity of RS-based GPP to increasing CO₂ and that implied by the emergent constraint. To do so, we develop a CO₂ sensitivity function for incorporating the effect of increasing CO₂ on the LUE of photosynthesis into satellite GPP estimates, based on the conservative assumption that the ecosystem-scale CO₂ sensitivity is consistent with that of the electron-transport limited rate of photosynthesis (A_j). This is supported by reports that the observed CO₂ response of photosynthesis and biomass closely corresponds to the CO₂-sensitivity of A_j (ref. 35). In addition, it has been suggested that shaded, and thus primarily electron-transport limited, leaves contribute the most canopy^{36,56} and global terrestrial photosynthesis³⁹. The assumption is further supported by optimal coordination theory, which posits that photosynthesis under typical daytime field conditions is close to the point where RuBisCO-limited (A_c) and A_j are colimiting. The colimitation of A_c and A_j has been shown to hold across a range of ecosystems⁵⁷, as has the downregulation of the maximum velocity of carboxylation (V_{cmax}) under

elevated CO₂ to maintain coordination⁵⁸. Given that the sensitivity of A_j to CO₂ is much smaller than that of A_c (ref. 59), the sensitivity of A_j to CO₂ therefore represents a conservative approach to incorporate a CO₂ sensitivity of LUE³⁷ in RS estimates of photosynthesis. Note that we also make the conservative assumption that C₄ plants operate at or near CO₂ saturation⁶⁰.

The mechanistic photosynthesis model proposed by ref. 49 captures the biochemical controls of leaf photosynthesis and responses to variations in temperature, light and CO₂ concentration. According to the model, the gross photosynthesis rate, A , is limited by either the capacity of the RuBisCO enzyme for the carboxylation of ribulose-1,5-bisphosphate (RuBP), the electron-transport capacity for RuBP regeneration. In the case of the limitation by the electron-transport capacity for RuBP regeneration, the photosynthetic rate (A_j , $\mu\text{mol m}^{-2} \text{s}^{-1}$) is given by:

$$A_j = \varphi_0 I \frac{c_i - \Gamma^*}{c_i + 2\Gamma^*} \quad (2)$$

where φ_0 is the intrinsic quantum efficiency, I is the absorbed light ($\mu\text{mol m}^{-2} \text{s}^{-1}$), c_i (Pa) is the leaf-internal CO₂ concentration and Γ^* (Pa) is the CO₂ compensation point. Parameter Γ^* depends on temperature, as estimated through a biochemical rate parameter (r)⁶¹:

$$\Gamma^* = r_{25} e^{\frac{\Delta H(T-298.15)}{298.15RT}} \quad (3)$$

where R is the molar gas constant ($8.314 \text{ J mol}^{-1} \text{ K}^{-1}$), $r_{25} = 4.22 \text{ Pa}$, is the photorespiratory point at 25 °C, ΔH is the activation energy for Γ^* ($37.83 \text{ kJ mol}^{-1}$) and T is the temperature in K. Assuming the CO₂ sensitivity of light-limited photosynthesis allows for the development of an index of the effect of CO₂ on photosynthetic LUE³⁷, which can be incorporated in any RS-based LUE model or empirical upscaling estimate of GPP.

By rewriting equation (2), substituting c_i by the product of atmospheric CO₂ (c_a) and the ratio of leaf-internal to leaf-ambient CO₂ ($\chi = c_i/c_a$), the sensitivity of GPP and LUE to CO₂ can be described as:

$$\begin{aligned} \frac{\partial \text{GPP}}{\partial \text{CO}_2} &= \frac{\partial \varphi_0 I \frac{c_a \chi - \Gamma^*}{c_a \chi + 2\Gamma^*}}{\partial \text{CO}_2}, \\ &= \varphi_0 I \frac{\partial \phi_{\text{CO}_2}}{\partial \text{CO}_2}, \\ &= > \frac{\partial \text{LUE}}{\partial \text{CO}_2} = \frac{\partial \phi_{\text{CO}_2}}{\partial \text{CO}_2} \end{aligned} \quad (4)$$

where $\phi_{\text{CO}_2} = \frac{c_a \chi - \Gamma^*}{c_a \chi + 2\Gamma^*}$ and $\text{LUE} = \text{GPP}/\varphi_0 I$. Note that the indirect effect of CO₂ on GPP through $\varphi_0 I$, is explicitly accounted for in satellite-based methods through changes in the fAPAR and considered here as an independent effect. However, the direct effect, through changes in LUE, (ϕ_{CO_2}), is not. We used equation (4) to derive a scalar, $f(\text{CO}_2)$, to account for the direct effect of CO₂ in any LUE-based estimate of GPP (for example, satellite or empirical upscaling approaches). To do so, we calculated ΔGPP in year t due to the effect of CO₂ on LUE as $\text{GPP}(t=0) \times f(\text{CO}_2)$, where:

$$f(\text{CO}_2) = \frac{(\phi_{\text{CO}_2}^t - \phi_{\text{CO}_2}^{1982})}{\phi_{\text{CO}_2}^{1982}} \quad (5)$$

$f(\text{CO}_2)$ thus represents the fractional increase in LUE due to the direct effect of CO₂ relative to a baseline period (here 1982, the start of the time series for the satellite-based methods considered).

The sensitivity of LUE to CO₂ thus depends on both Γ^* , which is calculated by means of equation (3), and χ . We estimated χ using the least-cost hypothesis^{19,62}. This states that an optimal long-term effective value of χ can be predicted as a result of plants minimizing their total

carbon costs associated with photosynthetic carbon gain and explicitly expressed with the following model:

$$\chi \approx \frac{\xi}{\xi + \sqrt{D}}, \text{ where } \xi = \sqrt{\frac{bK}{1.6\eta^*}} \quad (6)$$

where D is vapour pressure deficit and η^* is the viscosity of water relative to its value at 25 °C (ref. 63) and b is the ratio of the cost of maintaining carboxylation relative to that of maintaining transpiration¹⁹. The Michaelis–Menten coefficient of RuBisCO (K) is given by:

$$K = K_c \left(1 + \frac{P_o}{K_o} \right) \quad (7)$$

where K_c and K_o are the Michaelis–Menten coefficient of RuBisCO for carboxylation and oxygenation, respectively, expressed in partial pressure units and P_o is the partial pressure of O₂. K responds to temperature through K_c and K_o , the temperature responses for which are described using a temperature response function described by equation (3) with specific parameters: ΔH is 79.43 kJ mol⁻¹ for K_c and 36.38 kJ mol⁻¹ for K_o , r_{25} is 39.97 kPa for K_c and 27.48 kPa for K_o (ref. 61). We applied this derived sensitivity to the RS approaches detailed below, on a per-pixel basis in proportion to the percentage of C₃ plants in a given pixel⁶⁴, as C₄ plants operate at or near CO₂ saturation⁶⁰. We thus make the conservative assumption of no direct CO₂ effect on LUE in the C₄ proportion of each pixel.

Incorporating a CO₂ sensitivity into satellite-based GPP

The approach for incorporating a CO₂ sensitivity we outline above (equation (5)) can be incorporated into any satellite-based photosynthesis product. Here, we test it on two broadly used approaches. The first, the MODIS MOD17 algorithm (GPP_{MODIS} (ref. 65)) and the second an empirical upscaling method based on a model tree ensemble (GPP_{MTE} (ref. 66)). We applied the MODIS MOD17 GPP algorithm driven by 30-year (1982–2012) Global Inventory Modeling and Mapping Studies (GIMMS3g) fAPAR data⁶⁷, to calculate a new 30-year global monthly gridded (0.5°) dataset of MODIS-derived GPP:

$$\begin{aligned} \text{GPP}'_{\text{MODIS}} &= \text{GPP}_{\text{MODIS}} \times (1 + f(\text{CO}_2)) \\ &= \text{fAPAR} \times \text{PAR} \times \text{LUE}_{\text{max}} \times f(D) \times f(T_{\text{min}}) \times (1 + f(\text{CO}_2)) \quad (8) \\ &= \text{fAPAR} \times \text{PAR} \times \text{LUE} \end{aligned}$$

where LUE_{max} represents biome-specific maximum LUE, $f(D)$ represents a water stress reduction scalar based on the atmospheric vapour pressure deficit and $f(T_{\text{min}})$ represents a low-temperature stress reduction scalar. LUE_{max} , $f(D)$ and $f(T_{\text{min}})$ are parameterized according to ref. 68. Value $f(\text{CO}_2)$ is estimated on a per-pixel basis using equation (5). We used global monthly gridded (0.5°) weather data, provided by the Climate Research Unit at East Anglia University (CRU TS4.01). The total available photosynthetically active radiation (PAR) and D were calculated from insolation and CRU climate data using a simple process-based bioclimatic model (STASH⁶⁹).

To incorporate a CO₂ sensitivity in a global empirical upscaling dataset based on a model tree ensemble ML technique (GPP_{MTE}, 1982–2012⁶⁶), which does not account for the direct effect of CO₂ on LUE, we followed the approach outlined for the MODIS GPP product. Specifically, we applied the CO₂ function (equation (5)) to spatially distributed GPP_{MTE}, as:

$$\text{GPP}'_{\text{MTE}} = \text{GPP}_{\text{MTE}}(1 + f(\text{CO}_2)) \quad (9)$$

Early RS GPP models^{37,70} advocated for including a CO₂ effect on LUE, though primarily used the larger, light-saturated, sensitivity. A recent review⁷ found that the most widely used modern RS GPP

approaches^{65,66} do not include a CO₂ effect on LUE and of the 3 that did (out of 14 assessed) 2 are enzyme kinetics, not LUE, models (BESS⁷² and BEPS⁷⁰). The third (cFix⁷¹) assumes the light-saturated CO₂ sensitivity, which is not suitable for global application given the large contribution of RuBP regeneration-limited leaves^{36,73}. Some recent studies^{12,74,75} incorporated a CO₂ effect on LUE but the approach taken typically requires the reparameterization of the LUE model and is thus not easily applicable to other RS GPP products. The approach proposed here provides a generic and conservative method for incorporating CO₂ effects on LUE in any RS GPP product, which allows us to quantify the relative importance of incorporating a CO₂ effect in RS GPP products and reconciles the large difference between RS and TBM-derived sensitivities to CO₂.

Constraining terrestrial photosynthesis CO₂ sensitivity

Emergent constraints have gained prominence in recent years as a means by which to infer unobserved quantities of interest in land surface and climate models^{21–23}. The underlying core concept is that, although there is a large spread in the model estimates of an observed variable X and an unobserved variable Y across models, the relationship linking the two is sometimes tightly constrained across models. Given the existence of a strong and robust relationship across models between X and Y , observations of X can be used to generate a probabilistic inference, or constraint, on Y . This approach has been termed ‘emergent’ because the functional relationship cannot be diagnosed from a single model but rather emerges from examining the model spread^{21–23}.

The emergent constraint identified in this study links the sensitivity of GPP to CO₂ ($\beta_{\text{R}}^{\text{GPP}}$, see definition below) to the magnitude of the cumulative residual terrestrial sink (S_{LAND}) between 1982 and 2016. It is derived from a linear regression across an ensemble of TBMs between the modelled cumulative S_{LAND} and the sensitivity of GPP to CO₂. We use global simulations from 15 TBMs (Supplementary Table 2) run as part of the Trends in Net Land–Atmosphere Exchange (TRENDY v.6) initiative (<https://sites.exeter.ac.uk/trendy>) (v.6 data are reported in ref. 76). In TRENDY, common input forcing data were prescribed for a series of model experiments from 1901 to 2015. Here we use both the results of the TRENDY v.6 scenario S3 simulations (temporally dynamic climate, CO₂ and land use) as reported in the Global Carbon Project (GCP⁷⁶) and the TRENDY v.6 scenario S1 simulations (CO₂-only: temporally dynamic CO₂, time-invariant climate; pre-industrial land-use mask). For more details on the TRENDY project see ref. 24 and for details of the TRENDY v.6 simulations used here see ref. 76.

We estimated $\beta_{\text{R}}^{\text{GPP}}$ for each TRENDY v.6 TBM from annual GPP from the S1 (CO₂-only) simulations, performed by 15 models (Supplementary Table 2), using equation (1) over the 1982–2012 period (to maintain consistency with the RS methods assessed). Cumulative S_{LAND} (PgC) is calculated from the annual S_{LAND} (PgC yr⁻¹) reported by the GCP⁷⁶ for each TRENDY v.6 TBM, which represents the annual total net biome productivity plus emissions from land-use change.

The emergent constraint approach relies on a statistical relationship between a model predicted variable for which an observational constraint exists and one for which there is no observational constraint available^{21–23}. In the case of the relationship between $\beta_{\text{R}}^{\text{GPP}}$ and S_{LAND} , estimates of S_{LAND} are made annually by the Global Carbon Project, along with the associated uncertainties²⁵. The S_{LAND} values we use as the constraint are the cumulative reported annual values of the residual land sink from the Global Carbon Project²⁵ over the period from 1982 to 2016. Note that the period we used was chosen to both coincide with the satellite observations we use and to be sufficiently long so as to minimize the effect of macroclimatic events such as strong El Niño periods and volcanic eruptions.

The Global Carbon Project reports S_{LAND} uncertainty both on an annual, decadal and a cumulative basis, with an average uncertainty of 0.9 PgC yr⁻¹ for each of the four decades included in this study. For the

1960–2020 period where direct atmospheric CO₂ measurements are available, the Global Carbon Project estimates residual land carbon uptake of 135 ± 25 GtC (mean ± s.d.; ref. 25, Table 8), with a near-zero unattributed budget imbalance. The budget closure is interpreted as evidence of a coherent community understanding of the emissions and global sinks for this period²⁵. This provides a cumulative S_{LAND} reference uncertainty of 18.5%, which we apply to the cumulative fluxes of the period examined (1982 to 2016). It should be noted that the uncertainty on cumulative S_{LAND} is itself uncertain and is estimated by the Global Carbon Project based on the most up-to-date versions of the land surface models they use²⁵. Any future reduction in cumulative S_{LAND} uncertainty would decrease the uncertainty of β_R^{GPP} reported here.

Data availability

All data used to support the findings of this study are available publicly or on request. TRENDY model simulations are available on reasonable request from TRENDY coordinator S. Sitch (s.a.sitch@exeter.ac.uk; <https://globalcarbonbudgetdata.org/>). The Multivariate ENSO Index is available from <https://psl.noaa.gov/enso/mei/>. The GIMMS fAPAR data are available on request from R. Myneni, Boston University (<https://sites.bu.edu/cliveg/contact/>). Climate forcings used are available from Climate Research Unit at East Anglia University (<https://crudata.uea.ac.uk/cru/data/hrg/>). Upscaled GPP data are available from the FluxCom initiative of the Max Planck Institute for Biogeochemistry (<https://www.bgc-jena.mpg.de/geodb/projects/Home.php>).

Code availability

Code used to support the findings of this study is publicly available in the GitHub repository⁷⁷ at <https://github.com/trevorkeenan/gpp-co2-ncc>.

References

- Friedlingstein, P. et al. On the contribution of CO₂ fertilization to the missing biospheric sink. *Glob. Biogeochem. Cycles* **9**, 541–556 (1995).
- Farquhar, G. D., von Caemmerer, S. & Berry, J. A. A biochemical model of photosynthetic CO₂ assimilation in leaves of C₃ species. *Planta* **149**, 78–90 (1980).
- Myneni, R. B., Keeling, C. D., Tucker, C. J., Asrar, G. & Nemani, R. R. Increased plant growth in the northern high latitudes from 1981 to 1991. *Nature* **386**, 698–702 (1997).
- Zhu, Z. et al. Greening of the Earth and its drivers. *Nat. Clim. Change* **6**, 791–795 (2016).
- Keenan, T. F. et al. Increase in forest water-use efficiency as atmospheric carbon dioxide concentrations rise. *Nature* **499**, 324–327 (2013).
- Donohue, R. J., Roderick, M. L., McVicar, T. R. & Farquhar, G. D. Impact of CO₂ fertilization on maximum foliage cover across the globe's warm, arid environments. *Geophys. Res. Lett.* **40**, 3031–3035 (2013).
- Ukkola, A. M. et al. Reduced streamflow in water-stressed climates consistent with CO₂ effects on vegetation. *Nat. Clim. Change* **6**, 75–78 (2016).
- Smith, N. G. & Dukes, J. S. Plant respiration and photosynthesis in global-scale models: incorporating acclimation to temperature and CO₂. *Glob. Change Biol.* **19**, 45–63 (2013).
- De Kauwe, M. G. et al. A test of the 'one-point method' for estimating maximum carboxylation capacity from field-measured, light-saturated photosynthesis. *New Phytol.* **210**, 1130–1144 (2016).
- Maire, V. et al. The coordination of leaf photosynthesis links C and N fluxes in C₃ plant species. *PLoS ONE* **7**, e38345 (2012).
- Smith, N. G. & Keenan, T. F. Mechanisms underlying leaf photosynthetic acclimation to warming and elevated CO₂ as inferred from least-cost optimality theory. *Glob. Change Biol.* <https://doi.org/10.1111/gcb.15212> (2020).
- Lloyd, J. & Farquhar, G. The CO₂ dependence of photosynthesis, plant growth responses to elevated atmospheric CO₂ concentrations and their interaction with soil nutrient status. I. General principles and forest ecosystems. *Funct. Ecol.* **10**, 4–32 (1996).
- Ehleringer, J. & Björkman, O. Quantum yields for CO₂ uptake in C₃ and C₄ plants: dependence on temperature, CO₂ and O₂ concentration. *Plant Physiol.* **59**, 86–90 (1977).
- Bernacchi, C. J., Singsaas, E. L., Pimentel, C., Portis, A. R. Jr & Long, S. P. Improved temperature response functions for models of Rubisco-limited photosynthesis. *Plant Cell Environ.* **24**, 253–259 (2001).
- Wang, H. et al. Towards a universal model for carbon dioxide uptake by plants. *Nat. Plants* **3**, 734–741 (2017).
- Huber, M. L. et al. New international formulation for the viscosity of H₂O. *J. Phys. Chem. Ref. Data* **38**, 101–125 (2009).
- Still, C. J., Berry, J. A., Collatz, G. J. & DeFries, R. S. Global distribution of C₃ and C₄ vegetation: carbon cycle implications. *Glob. Biogeochem. Cycles* **17**, 6-1-6-14 (2003).
- Running, S. W. & Zhao, M. *Daily GPP and Annual NPP (MOD17A2/A3) Products NASA Earth Observing System MODIS Land Algorithm—User's Guide V3.28* (MODIS Land Team, 2015).
- Jung, M. et al. Global patterns of land-atmosphere fluxes of carbon dioxide, latent heat and sensible heat derived from eddy covariance, satellite and meteorological observations. *J. Geophys. Res.* <https://doi.org/10.1029/2010JG001566> (2011).
- Zhu, Z. et al. Global data sets of vegetation leaf area index (LAI)3g and fraction of photosynthetically active radiation (FPAR)3g derived from global inventory modeling and mapping studies (GIMMS) normalized difference vegetation index (NDVI3g) for the period 1981 to 2. *Remote Sens.* **5**, 927–948 (2013).
- Zhao, M. & Running, S. W. Drought-induced reduction in global terrestrial net primary production from 2000 through 2009. *Science* **329**, 940–943 (2010).
- Gallego-Sala, A. et al. Bioclimatic envelope model of climate change impacts on blanket peatland distribution in Great Britain. *Clim. Res.* **45**, 151–162 (2010).
- Veroustraete, F. On the use of a simple deciduous forest model for the interpretation of climate change effects at the level of carbon dynamics. *Ecol. Model.* **75–76**, 221–237 (1994).
- Jiang, C. & Ryu, Y. Multi-scale evaluation of global gross primary productivity and evapotranspiration products derived from Breathing Earth System Simulator (BESS). *Remote Sens. Environ.* **186**, 528–547 (2016).
- Zhang, S. et al. Evaluation and improvement of the daily boreal ecosystem productivity simulator in simulating gross primary productivity at 41 flux sites across Europe. *Ecol. Model.* **368**, 205–232 (2018).
- Liu, Y., Hejazi, M., Li, H., Zhang, X. & Leng, G. A hydrological emulator for global applications-HE v1.0.0. *Geosci. Model Dev.* **11**, 1077–1092 (2018).
- Yuan, W. et al. Increased atmospheric vapor pressure deficit reduces global vegetation growth. *Sci. Adv.* **5**, eaax1396 (2019).
- Cai, W. & Prentice, I. C. Recent trends in gross primary production and their drivers: analysis and modelling at flux-site and global scales. *Environ. Res. Lett.* **15**, 124050 (2020).
- Le Quéré, C. et al. Global Carbon Budget 2017. *Earth Syst. Sci. Data* **10**, 405–448 (2018).
- Keenan, T. F. GPP-CO₂: NCC paper code. *GitHub* github.com/trevorkeenan/gpp-co2-ncc (2023).

Acknowledgements

T.F.K. acknowledges support from NASA award 80NSSC21K1705, a US Department of Energy (DOE) ECRP Award DE-SC0021023, RUBISCO SFA DE-AC02-05CH11231 and the LEMONTREE project, funded through the generosity of E. Schmidt and W. Schmidt by

recommendation of the Schmidt Futures programme. T.F.K., X.L. and Y.Z. acknowledge additional support from the NASA IDS award NNH17AE86I. M.D.K. acknowledges support from the Australian Research Council (ARC) Centre of Excellence for Climate Extremes (CE170100023), the ARC Discovery Grant (DP190101823) and the NSW Research Attraction and Acceleration Program. I.C.P. acknowledges the Imperial College initiative on Grand Challenges in Ecosystems and the Environment and the European Research Council under the European Union's Horizon 2020 Research and Innovation Programme (grant agreement no. 787203 REALM). N.G.S. acknowledges support from Texas Tech University. B.D.S. was funded by the Swiss National Science Foundation grant no. PCEFP2_181115. C.T. was supported by a Lawrence Fellow award through Lawrence Livermore National Laboratory (LLNL), the DOE LLNL contract DE-AC52-07NA27344 and the LLNL-LDRD Program project 20-ERD-055. We thank R. Myneni and Z. Zhu for the provision of the fAPAR dataset, the Max Planck Institute for Biogeochemistry Department of Biogeochemical Integration for the provision of the upscaled GPP data. We thank the TRENDY team for the provision of the DGVM simulations and the researchers of the Global Carbon Project for making their data publicly available. We thank A. Walker for useful discussions on interpreting the deuterium isotopomer results and acknowledge the stimulating discussions during the Integrating CO₂ Fertilization Evidence Streams and Theory (ICOFEST) meeting September 2018, part of the FACE model Data-Synthesis project funded by the DOE, Office of Science, Office of Biological and Environmental Research. We thank P. Friedlingstein and C. Morfopoulos for valuable input on a previous version of this paper.

Author contributions

T.F.K. designed the study, performed the analysis and wrote the manuscript. X.L. aided in the regridding of the TRENDY model data. B.S. contributed to the emergent constraint implementation. M.D.K., B.S., I.C.P., W.H., N.S., B.M., X.L. and S.Z. provided feedback on the RS implementation. S.Z. and Y.Z. provided feedback on the emergent constraint implementation. B.S. provided feedback on the TRENDY model data interpretation. All authors discussed and commented on the results and the manuscript.

Competing interests

The authors declare no competing interests.

Additional information

Supplementary information The online version contains supplementary material available at <https://doi.org/10.1038/s41558-023-01867-2>.

Correspondence and requests for materials should be addressed to T. F. Keenan.

Peer review information *Nature Climate Change* thanks Sabrina Zechlau and the other, anonymous, reviewer(s) for their contribution to the peer review of this work.

Reprints and permissions information is available at www.nature.com/reprints.